



Contents lists available at ScienceDirect

Journal of King Saud University – Science

journal homepage: [www.sciencedirect.com](http://www.sciencedirect.com)

Original article

# Surface functionalization of mesoporous silica nanoparticles with Brønsted acids as a catalyst for esterification reaction

Amal Alfawaz<sup>1</sup>, Ali Alsalmeh<sup>1</sup>, Arwa Alkathiri, Abdullah Alswieleh<sup>\*</sup>

Department of Chemistry, College of Science, King Saud University, Riyadh, Saudi Arabia

## ARTICLE INFO

### Article history:

Received 6 January 2022

Revised 8 May 2022

Accepted 12 May 2022

Available online 18 May 2022

### Keywords:

Mesoporous silica nanoparticles

Surface functionalization

Brønsted acids

Catalysis

Esterification reaction

## ABSTRACT

This work presents the preparation of mesoporous silica nanoparticles (MSNs) using Stöber process. Then, the MSNs surface was modified with propyl thiol, followed by conversion of thiol to sulfonic acid using H<sub>2</sub>O<sub>2</sub>, acetic acid/H<sub>2</sub>O<sub>2</sub>, HNO<sub>3</sub>/H<sub>2</sub>O<sub>2</sub>, and H<sub>2</sub>SO<sub>4</sub>/H<sub>2</sub>O<sub>2</sub>. Surface modified MSNs were characterized by a variety of techniques: the Brunauer, Emmett and Teller (BET) technique, thermogravimetric analysis (TGA), scanning and transmission electron microscopies (SEM and TEM), dynamic light scattering (DLS) and Fourier-transform infrared spectroscopy (FTIR). The size of unmodified and modified MSNs ranged between 200 and 320 nm, with pore size of ca. 5.0 nm and surface area ca. 900 m<sup>2</sup>/g. The surface zeta potential was of the fabricated nanomaterials was estimated to be between –35 and –43 mV. When the surface modified MSNs were subjected to esterification reaction between heptanol and acetic acid, the conversion to ester reached 75% in the presence of MSNs-Pr-SO<sub>3</sub>H (via H<sub>2</sub>SO<sub>4</sub>/H<sub>2</sub>O<sub>2</sub>), comparing to MSNs-Pr-SO<sub>3</sub>H (via H<sub>2</sub>O<sub>2</sub>) or MSNs-Pr-SO<sub>3</sub>H (via Ac/H<sub>2</sub>O<sub>2</sub>). The conversion increased 75% to 93% for MSNs-Pr-SO<sub>3</sub>H (via H<sub>2</sub>SO<sub>4</sub>/H<sub>2</sub>O<sub>2</sub>) when the temperature increased from 90 °C to 110 °C, respectively.

© 2022 The Authors. Published by Elsevier B.V. on behalf of King Saud University. This is an open access article under the CC BY license (<http://creativecommons.org/licenses/by/4.0/>).

## 1. Introduction

Acids are very important compounds used widely as a catalyst agent in chemical industry. Sulfuric acid is one of the most important acid used in chemical industry (Clark, 2001). However, the use of such material in chemical industry is associated with wastewater production, equipment corrosion and complex product purification processes. Considerable attention has been paid to the use of solid acid catalysts due to their less-toxicity, ease of handling, environmental compatibility, waste reduction, reusability, and simplified products purification steps (Sheldon et al., 2007; Gupta and Paul, 2014). Solid acids (e.g. zeolites, heteropolyacids and acid polymers) are used as catalysts in many organic reactions in industrial areas such as oil refining (Vogt and Weckhuysen, 2015), biomass transformation (Liu et al., 2013), transesterification (Xie and Wang, 2013; Xie and Yang, 2011), biodiesel production

(Su and Guo, 2014; Lee and Wilson, 2015), and esterification (Pirez et al., 2014; Jeenpadiphat et al., 2015). However, many reports in the literature have been published on the development of high catalytic performance solid catalysts and as cost-effective as sulfuric acid (Alghamdi et al., 2020; Pan et al., 2022; Testa and La Parola, 2021).

Mesoporous silica nanoparticles (MSNs) have been used in different applications, including: sensors, environmental science and catalysis, due to their properties such as high surface area, regular pore shape, tunable pore size, large pore volume and excellent thermal stability (Lang et al., 2010; Mazloum-Ardakani et al., 2012; Xie et al., 2014; Alswieleh, 2020). Since the discovery of Mobil Composition of Matter No. 41 (MCM-41), it has been a great interest in the designing novel heterogeneous catalysts based on such materials (Thomas and Raja, 2008). Silica nanoparticles has the low acidity, comparing to mineral acids, thus it has been surface modification could be a good solution (Posada et al., 2010; Robles-Dutenhefner et al., 2009; Melero et al., 2012). Surface modification with organic functional groups has been rapidly developed to produce reusable organocatalysts (Zeidan et al., 2006; Li et al., 2004; Zeidan and Davis, 2007).

MSNs functionalized with sulfonic acid groups has been applied as an efficient Brønsted acid catalyst in biodiesel synthesis (Chen et al., 2011; Dhainaut et al., 2010; Shestakova et al., 2021), ethylene polymerization (Casas et al., 2012; Casas et al., 2013), glycerol

\* Corresponding author.

E-mail address: [aswieleh@ksu.edu.sa](mailto:aswieleh@ksu.edu.sa) (A. Alswieleh).

<sup>1</sup> These authors contributed equally.

Peer review under responsibility of King Saud University.



acetylation (Kim et al., 2014), and fatty acid esterification (Mar and Somsook, 2013; Mbaraka and Shanks, 2005). Chermahini et al. fabricated MSNs modified benzyl group and subsequently sulfonated by chlorosulfonic Acid (Chermahini et al., 2015). The fabricated nanomaterials were used to effectively catalyze the reaction between aryl nitriles and sodium azide to produce 5-aryl-1H-tetrazoles, comparing to a catalyst obtained from direct sulfonation of MSNs. Huang and co-workers reported the synthesis of bifunctionalized MSNs with site-separated Brønsted acids and bases: the internal surface modified with one group and the external surface of the MSNs modified with the second group (Huang et al., 2011). Both functional groups profomed as catalysts in two-step reaction sequence of 4-nitrobenzaldehyde dimethyl acetal and 4-nitrobenzaldehyde with nitromethane. Xue et al. reported the preparation of nanocatalyst made of sulfonic acid groups attached to mesoporous structure via a post-synthesis method for the synthesis of polyoxymethylene dimethyl ethers (PODE<sub>n</sub>) from methylal (DMM) and trioxymethylene (TOX) (Xue et al., 2017). The conversion rate of DMM and TOX to yield PODE<sub>2-8</sub> reached ~52, ~96, and ~62%, respectively, when a moderate amount of the nanocatalyst was added. Freire et al. reported the preparation of propyl- or aryl-sulfonic acid modified silica nanoparticles as effective catalysts in the esterification reactions (Aboelhassan et al., 2017). The catalysts demontated excellent catalytic performances in the esterification of linoleic acid with 100% conversion at 2 h reaction time, with reusability up to five catalytic cycles.

This work proposed to explore the effect of oxidation methods of thiol to sulfuric acid group on the catalytic activity of esterification reaction. Hence, mesoporous silica nanoparticles (MSNs) were fabricated in presence of cetyltrimethyl ammonium bromide (CTAB) as a template and expander (n-hexane) to produce porous nanostructured silica with pore size of ca. 5 nm and a relatively large surface area (ca. 900 m<sup>2</sup>/g) and size ranging between 200 and 320 nm. The MSNs surface was modified with propyl thiol, followed by conversion to sulfonic acid using several oxidizing agents such as H<sub>2</sub>O<sub>2</sub>, Ac/H<sub>2</sub>O<sub>2</sub> and H<sub>2</sub>SO<sub>4</sub>/H<sub>2</sub>O<sub>2</sub>. The nanocatalysts were subjected in the esterification reaction between heptanol and acetic acid. The nanocatalysts were characterized using physicochemical techniques such as the Brunauer, Emmett and Teller (BET) technique, thermogravimetric analysis (TGA), scanning and transmission electron microscopies (SEM and TEM), dynamic light scattering (DLS) and Fourier-transform infrared spectroscopy (FTIR).

## 2. Materials and methods

### 2.1. Materials

Tetraethyl orthosilicate (TEOS, 98%), hexadecyltrimethylammonium bromide (CTAB, 98), n-hexane (99%), dodecane (99%), ammonia aqueous (32 wt%), hydrochloric acid (35%), (3-mercaptopropyl) trimethoxysilane (MPTMS, 95%) and hydrogen peroxide (30%) were obtained from Sigma-Aldrich. hydrochloric acid (35%), methanol (99.8%), ethanol (96%), heptane (99%), toluene (99%), acetic acid (99.8%) sulfuric acid (98%) and nitric acid (65%) were purchased from Alfa Aesar.

### 2.2. Methods

#### 2.2.1. Preparation of mesoporous silica nanoparticles (MSNs)

Mesoporous silica nanoparticles were fabricated by placing 1 g of CTAB in a flask and dissolved in 160 mL of deionized water. Ammonia (7 mL) was added and left under magnetic stir until complete dissolving and became transparent. Then, a mixture of

20 mL n-hexane and 5 mL tetraethyl orthosilicate (TEOS) was added slowly, dropping drops into the solution. The solution turned from a transparent to a white suspension, then it is left for 12 h under continuous stirring. Then, the mixture was filtered with a Buechner funnel, washed several time with deionized water and methanol, and then dried in a drying oven for two hours at 120 °C (Alswieleh, 2020; Alswieleh, 2021).

CTAB/Silica nanoparticles were submitted to ion extraction to remove the CTAB. The nanomaterials were suspended in solution containing 10 mL of chloric acid and 160 mL of methanol at a temperature of 80 °C. The mixture was left for 12 h with constant stirring. After that, the solid was separated for by centrifuge at a speed of approximately 14,000 rpm, and washed washed several times with deionized water and ethanol.

#### 2.2.2. Preparation of mesoporous silica nanoparticles propyl sulfonic acid (MSNs-Pr-SO<sub>3</sub>H)

First, mesoporous silica nanoparticles functionalized thiol group (MSNs-Pr-thiol) were obtained by suspending 2 g of MSNs a mixture containing 50 mL of toluene and 0.5 mL of (3-mercaptopropyl)trimethoxysilane (MPTMS). The mixture was heated at a temperature of 120 °C under stirring. After 9 h, the solid is separated by centrifuge, then washed twice with toluene and five times with ethanol (Alswieleh, 2020).

Different methods have been used to convert thiol group to sulfonic acid group. First method, 1 g of MSNs-Pr-thiol was suspended in 30 mL of hydrogen peroxide (30%). The mixture was heated at 100 °C under stirring overnight. MSNs-Pr-SO<sub>3</sub>H (via H<sub>2</sub>O<sub>2</sub>) were separated by centrifugation and washed several times with water and ethanol, and dried at a temperature of 100 °C.

Second method, 1 g of MSNs-Pr-thiol was suspended in a mixture of 10 mL of acetic acid and 20 mL of hydrogen peroxide (30%). The mixture was heated at 100 °C under stirring overnight. MSNs-Pr-SO<sub>3</sub>H (via Ac/H<sub>2</sub>O<sub>2</sub>) were separated by centrifugation and washed several times with water and ethanol, and dried at a temperature of 100 °C.

Third method, 1 g of MSNs-Pr-thiol was suspended in 30 mL of hydrogen peroxide and concentrated nitric acid (0.5 mL). The mixture was stirred for 12 h. MSNs-Pr-SO<sub>3</sub>H (via HNO<sub>3</sub>/H<sub>2</sub>O<sub>2</sub>) were separated by centrifugation and washed several times with water and ethanol, and dried at a temperature of 100 °C.

Fourth method, 1 g of MSNs-Pr-thiol was suspended in a mixture 30 mL of hydrogen peroxide (30%) and concentrated sulfuric acid (0.5 mL). The mixture was stirred overnight. MSNs-Pr-SO<sub>3</sub>H (via H<sub>2</sub>SO<sub>4</sub>/H<sub>2</sub>O<sub>2</sub>) were separated by centrifugation and washed several times with water and ethanol, and dried at a temperature of 100 °C.

### 2.3. Measurement and characterization

Fourier Transform Infrared (FT-IR) instrument from PerkinElmer, spectrum BX was utilized to obtain IR spectra, with a range of 4000–400 cm<sup>-1</sup> with a resolution of 4 cm<sup>-1</sup>. Surface area analysis was performed with an ASAP 2020 instrument manufactured by micromeritics. The samples were analyzed by thermogravimetric analysis instrument (TGA) made by a PerkinElmer, at temperature range from 22 °C to 800 °C at a heating rate of 10 °C per minute. Transmission Electron Microscopy from JEOL (JEM-1400Plus) was used to image the samples. JSM-7610F Scanning Electron Microscopy instrument was also used to image the samples. The products of esterification reactions was analyzed using a gas chromatography instrument (GC), with a flame ionization detector (FID) and helium gas at te temperature between 50 and 200 °C.

### 3. Results and discussion

Scanning electron microscopy (SEM) and transmission electron microscopy (TEM) were utilized to acquire morphological image of the nanostructure materials. As illustrated in Fig. 1a, the mesoporous silica nanoparticles shape was almost spherical with size between 210 and 380 nm. The average particle size was 280 nm, as estimated to be imageJ software. TEM image illustrates that the particles size was between 200 nm and 310 nm, with clear pore structure (Fig. 1B). The average pores size was estimated to be 5 nm.

To demonstrate the successful attachment of silane molecules on MSNs surface, FTIR spectra were recorded for MSNs (as made), CTAB-free MSNs, and MSNs-Pr-SH, shown in Fig. 2A. In all samples, a wide band was noticed between 1250 and 1050  $\text{cm}^{-1}$  for Si–O–Si band stretching in silica, and stretching vibration of Si–O at ca. 800  $\text{cm}^{-1}$ . For as-made MSNs sample, peaks at ca. 2900  $\text{cm}^{-1}$

and 1450  $\text{cm}^{-1}$  were observed, which were referred to C–H stretching vibration and C–H bending vibration of CTAB molecules. The successful removal of CTAB was approved by disappearance of C–H stretching and bending vibrations. After attachment of silane molecules, new peaks were observed at ca. 1450  $\text{cm}^{-1}$  and 2900  $\text{cm}^{-1}$ , which were appointed to C–H bending and stretching vibrations, respectively in propyl moieties. No difference in FTIR spectra was observed after conversion thiol group to sulphonic acid group (data not presented) (Alswieleh, 2021; Alswieleh et al., 2021). The fabricated samples were analyzed using thermogravimetric analysis (TGA) technique, Fig. 2B. It was noticed that the weight loss of CTAB free MSNs was ca. 5% at  $\sim 800$   $^{\circ}\text{C}$ , which could be related to the detachment of water molecules from the surface. After salinization process, the amount loss was approximately 12% for all samples, which referred to organic layers. Such weight loss indicated the successful attachment of organosilane self-assembled monolayers on the surface.

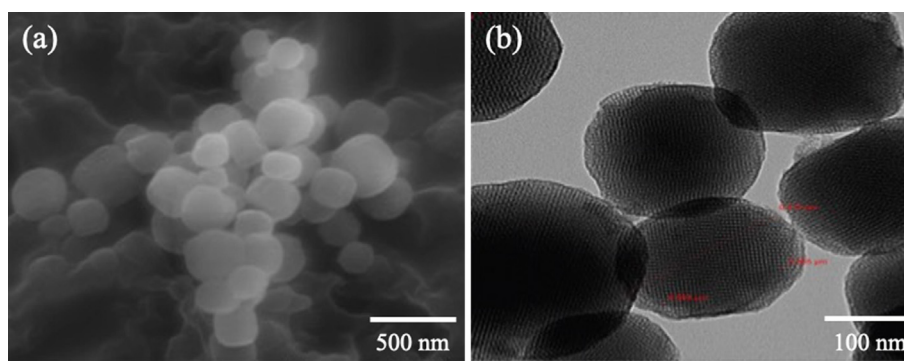


Fig. 1. Illustration of (a) SEM image of MSNs. (b) TEM image of MSNs.

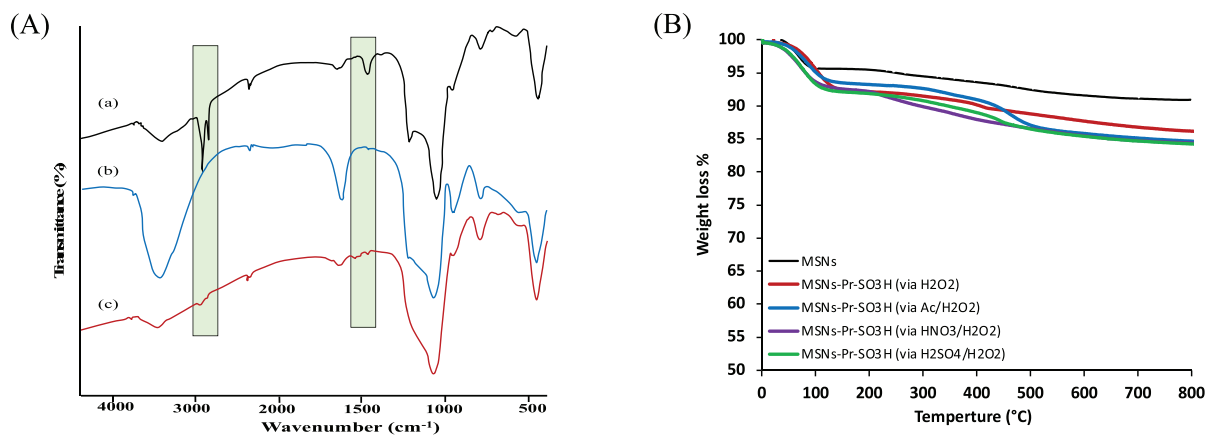
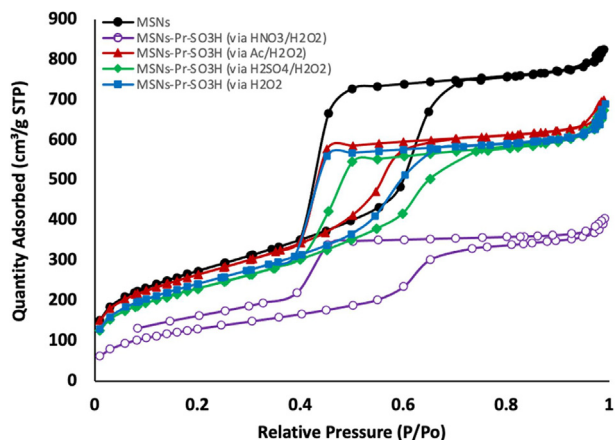


Fig. 2. (A) FTIR spectra of the fabricated nanoparticles: (a) as-made MSNs, (b) template free MSNs and (c) MSNs-Pr-SH. (B) Thermogravimetric analysis (TGA) of the fabricated nanoparticles: (black) CTAB free MSNs, (red) MSNs-Pr-SO<sub>3</sub>H (via H<sub>2</sub>O<sub>2</sub>), (blue) MSNs-Pr-SO<sub>3</sub>H (via Ac/H<sub>2</sub>O<sub>2</sub>), (purple) MSNs-Pr-SO<sub>3</sub>H (via HNO<sub>3</sub>/H<sub>2</sub>O<sub>2</sub>), and (green) MSNs-Pr-SO<sub>3</sub>H (via H<sub>2</sub>SO<sub>4</sub>/H<sub>2</sub>O<sub>2</sub>).

Table 1

Shows the surface area, pore size and pore volume of the prepared nanomaterials.

Sample	S <sub>BET</sub> (m <sup>2</sup> /g)	Pore size (nm)	Pore Volume (cm <sup>3</sup> /g)
CTAB free MSNs	971	5.2	1.28
MSNs-Pr-SO <sub>3</sub> H (via H <sub>2</sub> O <sub>2</sub> )	784	4.7	0.98
MSNs-Pr-SO <sub>3</sub> H (via Ac/H <sub>2</sub> O <sub>2</sub> )	864	4.9	1.06
MSNs-Pr-SO <sub>3</sub> H (via HNO <sub>3</sub> /H <sub>2</sub> O <sub>2</sub> )	672	3.9	0.83
MSNs-Pr-SO <sub>3</sub> H (via H <sub>2</sub> SO <sub>4</sub> /H <sub>2</sub> O <sub>2</sub> )	823	5.0	1.04



**Fig. 3.** Brunauer-Emmett-Teller (BET) surface area analysis of the fabricated nanoparticles: (black) CTAB free MSNs, (blue) MSNs-Pr-SO<sub>3</sub>H (via H<sub>2</sub>O<sub>2</sub>), (red) MSNs-Pr-SO<sub>3</sub>H (via Ac/H<sub>2</sub>O<sub>2</sub>), (purple) MSNs-Pr-SO<sub>3</sub>H (via HNO<sub>3</sub>/H<sub>2</sub>O<sub>2</sub>), and (green) MSNs-Pr-SO<sub>3</sub>H (via H<sub>2</sub>SO<sub>4</sub>/H<sub>2</sub>O<sub>2</sub>).

Brunauer-Emmett-Teller (BET) surface area analysis was also utilized to study change in the surface after organic layers attachment, (Table 1 and Fig. 3). The results illustrated that all samples have a relative large surface area between 680 and 950 m<sup>2</sup>/g, and the pore size ranged between 3.8 and 5.2 nm, (Table 1). The surface area of free template nanoparticles was 971 m<sup>2</sup>/g, with pore size of 1.28 nm. The surface area, pore size and pore volume were decreased when surface had been modified with organosilane

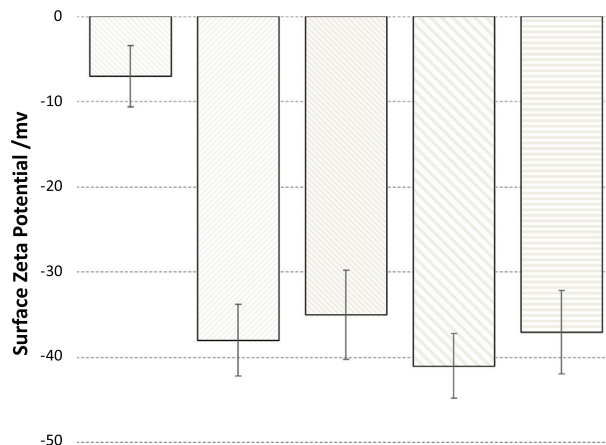


**Fig. 4.** Surface zeta potential of surface modified MSNs in deionized water.

self-assembled monolayers. Such reductions indicated the successful attachment of organic layers.

As shown in Fig. 3, the N<sub>2</sub> sorption isotherms were found to be Type IV for all fabricated samples which is related to mesoporous nature. A considerable change in capillary condensation steps at higher relative pressures between nonmodified and modified nanoparticles were observed. Such change in the hysteresis loop suggested that the pore sizes and shapes had been changed.

Surface zeta potential of MSNs-Pr-SH and MSNs-Pr-SO<sub>3</sub>H were determined using dynamic light scattering (DLS). The surface zeta

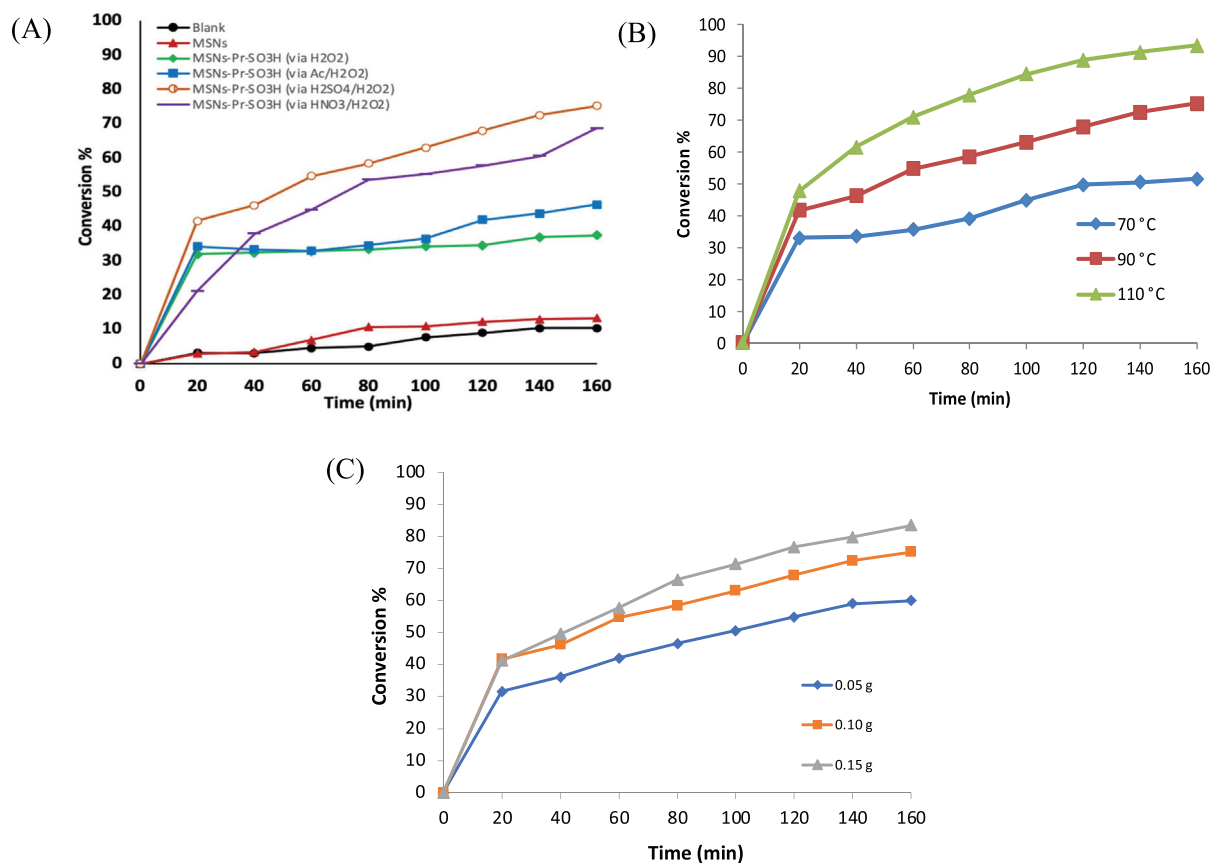


**Fig. 5.** (A) The conversion in the esterification reaction of acetic acid with heptanol at 90 °C and in the presence of: (black) blank, (red) MSNs, (green) MSNs-Pr-SO<sub>3</sub>H (via H<sub>2</sub>O<sub>2</sub>), (blue) MSNs-Pr-SO<sub>3</sub>H (via Ac/H<sub>2</sub>O<sub>2</sub>), (orange) MSNs-Pr-SO<sub>3</sub>H (via HNO<sub>3</sub>/H<sub>2</sub>O<sub>2</sub>), and (purple) MSNs-Pr-SO<sub>3</sub>H (via H<sub>2</sub>SO<sub>4</sub>/H<sub>2</sub>O<sub>2</sub>). (B) The conversion in the esterification reaction of acetic acid with heptanol using MSNs-Pr-SO<sub>3</sub>H (via H<sub>2</sub>SO<sub>4</sub>/H<sub>2</sub>O<sub>2</sub>) at different temperature. (C) The conversion in the esterification reaction of acetic acid with heptanol using MSNs-Pr-SO<sub>3</sub>H (via H<sub>2</sub>SO<sub>4</sub>/H<sub>2</sub>O<sub>2</sub>) at different mass of the catalyst at 90 °C.

potential of MSNs-Pr-SH was found to be around  $-10$  mV. After oxidation, the surface zeta became in range between  $-35$  and  $-42$  mV, due to the conversion of thiol groups to sulfonic acid groups (permanent negative charged) on the MSNs surfaces, (Fig. 4).

A series of esterification reactions were carried out using  $0.1$  g of the fabricated nanomaterials at different time and  $90$  °C. The total mass of the reaction mixture was  $10$  g; acetic acid and heptanol with molar ratio of  $1:5$ , respectively, in the presence of  $0.2$  g dodecane, as a standard. The conversion percentage was determined by dividing the number of moles of the acid remaining in the reaction mixture to the number of moles of the reacted acid.

Fig. 5A illustrates the conversion in the esterification reaction of acetic acid with heptanol in presence of MSNs, MSNs-Pr-SO<sub>3</sub>H (via H<sub>2</sub>O<sub>2</sub>), MSNs-Pr-SO<sub>3</sub>H (via Ac/H<sub>2</sub>O<sub>2</sub>), MSNs-Pr-SO<sub>3</sub>H (via HNO<sub>3</sub>/H<sub>2</sub>O<sub>2</sub>), and MSNs-Pr-SO<sub>3</sub>H (via H<sub>2</sub>SO<sub>4</sub>/H<sub>2</sub>O<sub>2</sub>). The conversion reached  $10\%$  after  $160$  min from the start of the reaction in the absence of the catalyst (Blank). Similar behavior was observed when MSNs was added. It was observed that the conversion increased after oxidation thiol group. The conversion was ca.  $40\%$  in the presence of either MSNs-Pr-SO<sub>3</sub>H (via H<sub>2</sub>O<sub>2</sub>) or MSNs-Pr-SO<sub>3</sub>H (via Ac/H<sub>2</sub>O<sub>2</sub>). The highest conversion was ca.  $75\%$  when H<sub>2</sub>SO<sub>4</sub>/H<sub>2</sub>O<sub>2</sub> was used in the thiol oxidation process.

Several reactions were carried out on esterification reaction with changing the temperatures and the mass of the MSNs-Pr-SO<sub>3</sub>H (via H<sub>2</sub>SO<sub>4</sub>/H<sub>2</sub>O<sub>2</sub>). It is clearly that when the reaction temperature is increased, the conversion to an ester increases. When the temperature was changed from  $70$  °C,  $90$  °C to  $110$  °C, the conversion rate increased from  $52\%$ ,  $75\%$  and  $93\%$ , respectively, as shown in Fig. 5B. Moreover, it was found that there is a direct relationship between the conversion and the amount of catalyst. The conversion increased from  $60\%$ ,  $75\%$ , and  $84\%$ , when the mass of the catalyst increased from  $0.05$  g,  $0.1$  g, and  $0.15$  g (Fig. 5C).

#### 4. Conclusions

MSNs were synthesized using CTAB as a template to produce porous nanomaterials, size ranging between  $200$  and  $320$  nm with a relatively large surface area ( $\sim 900$  m<sup>2</sup>/g), and a pore size of  $\sim 5.0$  nm. The MSNs surface was modified with propyl thiol, followed by conversion of thiol to sulfonic acid using several methods. The nanomaterials have been characterized by a variety of techniques such as FT-IR, TGA, SEM, TEM and BET. The results of the analysis showed that the fabricated nanoparticles had good thermal stability. The nanocatalysts were subjected in the esterification reaction, consisting of acetic acid and heptanol. The conversion reached  $40\%$  in the presence of either MSNs-Pr-SO<sub>3</sub>H (via H<sub>2</sub>O<sub>2</sub>) or MSNs-Pr-SO<sub>3</sub>H (via Ac/H<sub>2</sub>O<sub>2</sub>), comparing to  $10\%$  for MSNs. The highest conversion was observed for MSNs-Pr-SO<sub>3</sub>H (via H<sub>2</sub>SO<sub>4</sub>/H<sub>2</sub>O<sub>2</sub>) with  $75\%$  conversion. The conversion increased up to  $93\%$  for MSNs-Pr-SO<sub>3</sub>H (via H<sub>2</sub>SO<sub>4</sub>/H<sub>2</sub>O<sub>2</sub>) when the temperature was changed to  $110$  °C. Moreover, the conversion increased from  $75\%$  at  $0.1$  g of MSNs-Pr-SO<sub>3</sub>H (via H<sub>2</sub>SO<sub>4</sub>/H<sub>2</sub>O<sub>2</sub>) to  $84\%$ , at  $0.15$  g of the catalyst.

#### Funding

This research received no external funding.

#### Acknowledgements

This research was supported by Researchers Supporting Project number (RSP-2021/238) from King Saud University, Riyadh, Saudi Arabia.

#### Conflicts of Interest

The authors declare that they have no conflicts of interest.

#### References

- Abuelhassan, M.M., Peixoto, A.F., Freire, C., 2017. Sulfonic acid functionalized silica nanoparticles as catalysts for the esterification of linoleic acid. *New J. Chem.* 41 (9), 3595–3605.
- Alghamdi, A.A., Mrair, Y.M., Alharthi, F.A., Al-Odayni, A.-B., 2020. Catalytic Performance of SBA-15-Supported Poly (Styrenesulfonic Acid) in the Esterification of Acetic Acid with n-Heptanol. *Appl. Sci.* 10 (17), 5835.
- Alswieleh, A.M., 2020. Modification of Mesoporous Silica Surface by Immobilization of Functional Groups for Controlled Drug Release. *J. Chem.* 2020, 1–9.
- Alswieleh, A.M., 2021. Remediation of cationic and anionic dyes from water by histidine modified mesoporous silica. *Int. J. Environ. Anal. Chem.*, 1–13
- Alswieleh, A.M., 2021. Cysteine-and glycine-functionalized mesoporous silica as adsorbents for removal of paracetamol from aqueous solution. *Int. J. Environ. Anal. Chem.*, 1–12
- Alswieleh, A.M., Albahar, H.Y., Alfawaz, A.M., Alsilmeh, A.S., Beagan, A.M., Alsalmeh, A. M., Almeataq, M.S., Alshahrani, A., Alotaibi, K.M., Nishikiori, H., 2021. Evaluation of the Adsorption Efficiency of Glycine-, Iminodiacetic Acid-, and Amino Propyl-Functionalized Silica Nanoparticles for the Removal of Potentially Toxic Elements from Contaminated Water Solution. *J. Nanomater.* 2021, 1–12.
- Casas, E., van Grieken, R., Escola, J., 2012. Polymerization of ethylene with (nBuCp) 2ZrCl<sub>2</sub> supported over mesoporous SBA-15 functionalized with sulfonic acid groups. *Appl. Catal. A* 437, 44–52.
- Casas, E., Paredes, B., Van Grieken, R., 2013. (n BuCp) 2 ZrCl 2 supported over mesoporous propyl sulfonic silica-alumina: a highly active heterogeneous catalyst for ethylene polymerization. *Catal. Sci. Technol.* 3 (10), 2565–2570.
- Chen, S.-Y., Yokoi, T., Tang, C.-Y., Jang, L.-Y., Tatsumi, T., Chan, J.C., Cheng, S., 2011. Sulfonic acid-functionalized platelet SBA-15 materials as efficient catalysts for biodiesel synthesis. *Green Chem.* 13 (10), 2920–2930.
- Chermahini, A.N., Omran, M.K., Dabbagh, H.A., Mohammadnezhad, G., Teimouri, A., 2015. Application of a functionalized mesoporous silica catalyst to the synthesis of tetrazoles. *New J. Chem.* 39 (6), 4814–4820.
- Clark, J.H., 2001. Catalysis for green chemistry. *Pure Appl. Chem.* 73 (1), 103–111.
- Dhainaut, J., Dacquain, J.-P., Lee, A.F., Wilson, K., 2010. Hierarchical macroporous-mesoporous SBA-15 sulfonic acid catalysts for biodiesel synthesis. *Green Chem.* 12 (2), 296–303.
- Gupta, P., Paul, S., 2014. Solid acids: Green alternatives for acid catalysis. *Catal. Today* 236, 153–170.
- Huang, Y., Xu, S., Lin, V.S.Y., 2011. Bifunctionalized Mesoporous Materials with Site-Separated Brønsted Acids and Bases: Catalyst for a Two-Step Reaction Sequence. *Angew. Chem. Int. Ed.* 50 (3), 661–664.
- Jeenpadiphat, S., Björk, E.M., Odén, M., Tungasmita, D.N., 2015. Propylsulfonic acid functionalized mesoporous silica catalysts for esterification of fatty acids. *J. Mol. Catal. A: Chem.* 410, 253–259.
- Kim, I., Kim, J., Lee, D., 2014. A comparative study on catalytic properties of solid acid catalysts for glycerol acetylation at low temperatures. *Appl. Catal. B* 148, 295–303.
- Lang, L., Li, B., Liu, W., Jiang, L., Xu, Z., Yin, G., 2010. Mesoporous ZnS nanospheres: a high activity heterogeneous catalyst for synthesis of 5-substituted 1 H-tetrazoles from nitriles and sodium azide. *Chem. Commun.* 46 (3), 448–450.
- Lee, A.F., Wilson, K., 2015. Recent developments in heterogeneous catalysis for the sustainable production of biodiesel. *Catal. Today* 242, 3–18.
- Li, H., Zhou, B., Lin, Y., Gu, L., Wang, W., Fernando, K.S., Kumar, S., Allard, L.F., Sun, Y.-P., 2004. Selective interactions of porphyrins with semiconducting single-walled carbon nanotubes. *J. Am. Chem. Soc.* 126 (4), 1014–1015.
- Liu, F., Zheng, A., Noshadi, I., Xiao, F.-S., 2013. Design and synthesis of hydrophobic and stable mesoporous polymeric solid acid with ultra strong acid strength and excellent catalytic activities for biomass transformation. *Appl. Catal. B* 136, 193–201.
- Mar, W.W., Somsook, E., 2013. Esterification of fatty acid catalyzed by hydrothermally stable propylsulfonic acid-functionalized mesoporous silica SBA-15. *J. Oleo Sci.* 62 (6), 435–442.
- Mazloum-Ardakani, M., Sheikh-Mohseni, M.A., Abdollahi-Alibeik, M., Benvidi, A., 2012. Application of nanosized MCM-41 to fabrication of a nanostructured electrochemical sensor for the simultaneous determination of levodopa and carbidopa. *Analyst* 137 (8), 1950–1955.
- Mbaraka, I.K., Shanks, B.H., 2005. Design of multifunctionalized mesoporous silicas for esterification of fatty acid. *J. Catal.* 229 (2), 365–373.
- Melero, J.A., Vicente, G., Paniagua, M., Morales, G., Muñoz, P., 2012. Etherification of biodiesel-derived glycerol with ethanol for fuel formulation over sulfonic modified catalysts. *Bioresour. Technol.* 103 (1), 142–151.
- Pan, H., Xia, Q., Li, H., Wang, Y., Shen, Z., Wang, Y., Li, L., Li, X., Xu, H., Zhou, Z., 2022. Direct production of biodiesel from crude Euphorbia lathyris L. Oil catalyzed by multifunctional mesoporous composite materials. *Fuel* 309, 122172.
- Pirez, C., Lee, A., Manayil, J.C., Parlett, C., Wilson, K., 2014. Hydrothermal saline promoted grafting: a route to sulfonic acid SBA-15 silica with ultra-high acid site loading for biodiesel synthesis. *Green Chem.* 16 (10), 4506–4509.

- Posada, J.A., Cardona, C.A., Giraldo, O., 2010. Comparison of acid sulfonic mesostructured silicas for 1-butylacetate synthesis. *Mater. Chem. Phys.* 121 (1–2), 215–222.
- Robles-Dutenhefner, P.A., da Silva Rocha, K.A., Sousa, E.M., Gusevskaya, E.V., 2009. Cobalt-catalyzed oxidation of terpenes: Co-MCM-41 as an efficient shape-selective heterogeneous catalyst for aerobic oxidation of isolongifolene under solvent-free conditions. *J. Catal.* 265 (1), 72–79.
- Sheldon, R.A., Arends, I.W.C.E., Hanefeld, U. (Eds.), 2007. *Green Chemistry and Catalysis*. Wiley.
- Shestakova, P., Popova, M., Szegedi, A., Lazarova, H., Luong, T.K.N., Trendafilova, I., Mihály, J., Parac-Vogt, T.N., 2021. Hybrid catalyst with combined Lewis and Brønsted acidity based on ZrIV substituted polyoxometalate grafted on mesoporous MCM-41 silica for esterification of renewable levulinic acid. *Micropor. Mesopor. Mater.* 323, 111203.
- Su, F., Guo, Y., 2014. Advancements in solid acid catalysts for biodiesel production. *Green Chem.* 16 (6), 2934–2957.
- Testa, M.L., La Parola, V., 2021. Sulfonic Acid-Functionalized Inorganic Materials as Efficient Catalysts in Various Applications: A Minireview. *Catalysts* 11 (10), 1143.
- Thomas, J.M., Raja, R., 2008. Exploiting nanospace for asymmetric catalysis: confinement of immobilized, single-site chiral catalysts enhances enantioselectivity. *Acc. Chem. Res.* 41 (6), 708–720.
- Vogt, E.T., Weckhuysen, B.M., 2015. Fluid catalytic cracking: recent developments on the grand old lady of zeolite catalysis. *Chem. Soc. Rev.* 44 (20), 7342–7370.
- Xie, T., Shi, L., Zhang, J., Zhang, D., 2014. Immobilizing Ni nanoparticles to mesoporous silica with size and location control via a polyol-assisted route for coking-and sintering-resistant dry reforming of methane. *Chem. Commun.* 50 (55), 7250–7253.
- Xie, W., Wang, T., 2013. Biodiesel production from soybean oil transesterification using tin oxide-supported WO<sub>3</sub> catalysts. *Fuel Process. Technol.* 109, 150–155.
- Xie, W., Yang, D., 2011. Silica-bonded N-propyl sulfamic acid used as a heterogeneous catalyst for transesterification of soybean oil with methanol. *Bioresour. Technol.* 102 (20), 9818–9822.
- Xue, Z., Shang, H., Xiong, C., Lu, C., An, G., Zhang, Z., Cui, C., Xu, M., 2017. Synthesis of polyoxymethylene dimethyl ethers catalyzed by sulfonic acid-functionalized mesoporous SBA-15. *RSC Adv.* 7 (33), 20300–20308.
- Zeidan, R.K., Davis, M.E., 2007. The effect of acid–base pairing on catalysis: An efficient acid–base functionalized catalyst for aldol condensation. *J. Catal.* 247 (2), 379–382.
- Zeidan, R.K., Dufaud, V., Davis, M.E., 2006. Enhanced cooperative, catalytic behavior of organic functional groups by immobilization. *J. Catal.* 239 (2), 299–306.